WET OXIDATION OF GLYCEROL INTO FINE ORGANIC ACIDS: CATALYST SELECTION AND KINETIC EVALUATION

J. E. N. Brainer[1*], D. C. S. Sales[1], E. B. M. Medeiros[2], N. M. Lima Filho[1] and
C. A. M. Abreu[1]

[1]Universidade Federal de Pernambuco, Laboratório de Processos Catalíticos, LPC, Departamento
de Engenharia Química, Universidade Federal de Pernambuco, 50740-520, Recife - PE, Brazil.
Phone: + 55 (81) 94088082, Fax: +55 (81) 2126-7289
*E-mail: netoqmc@yahoo.com.br
E-mail: deivsoncesar@yahoo.com.br, med@ufpe.br, cesar@ufpe.br
[2]Universidade Federal da Paraíba, Centro de Tecnologia de Desenvolvimento Regional,
Campus I, 58051-900, João Pessoa - PB, Brazil.

Abstract - The liquid phase oxidation of glycerol was performed producing fine organic acids. Catalysts based on Pt, Pd and Bi supported on activated carbon were employed to perform the conversion of glycerol into organic acids at 313 K, 323 K and 333 K, under atmospheric pressure (1.0 bar), in a mechanically agitated slurry reactor (MASR). The experimental results indicated glycerol conversions of 98% with production of glyceric, tartronic and glycolic acids, and dihydroxyacetone. A yield of glyceric acid of 69.8%, and a selectivity of this compound of 70.6% were reached after 4 h of operation. Surface mechanisms were proposed and rate equations were formulated to represent the kinetic behavior of the process. Selective formation of glyceric acid was observed, and the kinetic parameter values indicated the lowest activation energy (38.5 kJ/mol) for its production reaction step, and the highest value of the adsorption equilibrium constant of the reactant glycerol (10^{-4} dm^3/mol).
Keywords: Glycerol oxidation; Catalysts; Glyceric acid; Kinetics; Modeling.

INTRODUCTION

Glycerol is an important renewable resource derived from biomass and is currently used in pharmaceutical, food and cosmetics applications (Corma *et al*., 2007; Luo *et al*., 2008; Ferretti *et al*., 2010; Lehr *et al*., 2007; Guo *et al*., 2009). The conversion of glycerol is of interest because it is a byproduct of biodiesel production from plant and animal oils (Tullo, 2007). The rapid expansion of biodiesel production capacity around the world has caused a major surplus of glycerol (McCoy, 2006).

This increasing production of biodiesel has resulted in a price decline of crude glycerol, making aqueous glycerol an attractive compound for the synthesis of fine chemicals (Behr *et al*., 2008).

A range of possible products can be derived from glycerol oxidation, such as dihydroxyacetone (DHA), hydroxypyruvic acid (HPA), glyoxalic acid (GOX), oxalic acid (OXA), glyceraldehyde (GLA), glyceric acid (GCA), and tartronic acid (TTA) (Fordham *et al*., 1996). Glyceric acid and dihydroxyacetone are the main products obtained from glycerol oxidation in the presence of palladium and platinum catalysts

---

(Mallat and Baiker, 1995; Kimura et al., 1993; Kimura, 1993; Fordham et al., 1996). Tartronic acid and oxalic acid are also formed by oxidation of glyceric acid and dihydroxyacetone (Fordham et al., 1996; Worz, 2009). An increasing number of studies on oxidation of glycerol with oxygen in aqueous solution have been conducted with catalysts based on palladium and platinum (Kimura et al., 1993; Kimura, 1993; Fordham et al., 1996). The addition of bismuth as a promoter incorporated to the palladium and platinum catalysts had an influence on the catalyst selectivity (Alardin et al., 2001). The mechanism of glycerol oxidation on theses catalysts has been shown to involve oxidative dehydrogenation. Thus, it was observed that the presence of NaOH was important for the initiation of the catalytic glycerol oxidation (Carrettin et al., 2001; Demirel et al., 2005; Ketchie et al., 2007; Ketchie et al., 2007).

The knowledge of a phenomenological kinetic model that can correctly predict the transformation of glycerol will be useful for selection of operating conditions depending on the desired goal. Phenomenological models to represent experimental results of glycerol oxidation, in order to obtain selective organic acids, have been proposed, (Ketchie et al., 2007; Demirel et al., 2007).

The purpose of this work was to develop the catalytic oxidation of glycerol in alkaline media in the presence of platinum, palladium and bismuth catalysts supported on activated carbon with different metal compositions. The selectivity of the process was evaluated in terms of the main products glyceric and tartronic acids. The experimental evidences allowed the formulation of a reaction scheme based on kinetic modeling according to the Langmuir-Hinshelwood approach.

EXPERIMENTAL

Catalyst Preparation

The carbon-supported catalysts were prepared by wet impregnation, followed by calcination and reduction. The choice of the method was due to indications of oxidation activities for glycerol conversion (Verde et al., 2004; Gallezot, 1997). The catalysts were formulated based on the following compositions: Pt(3.0 wt.%)/C and Pd(0.2 wt.%)-Pt(1.0 wt.%)-Bi(2.0 wt.%)/C. The activated carbon (Ref. C-119) used as support was from Carbomafra (Brazil). The pH was adjusted to values above or below the isoelectric point of activated carbon, about 6.8, due

to the need to incorporate metal in the form of anions or cations during impregnation.

The salts $H_2PtCl_6 \cdot 6H_2O$ (>99%) and $Bi(NO_3)3.5H_2O$ (>98%) were supplied by VETEC (Brazil) and $PtCl_2$ (99.99%) and $PdCl_2$(99.99%) were supplied by Acros Organics. Glyceric acid (GCA, 99.9%) and 1,3-dihydroxyacetone dimer (DHA, 97%) were obtained from Sigma-Aldrich Corporation (USA), tartronic acid (TTA, 98%) from ALFA AESAR (USA), glycolic acid (GLYCA, 70 wt.% in water) and oxalic acid (OXA, 99.9%) from VETEC (Brazil)."

The platinum catalyst was prepared by wet impregnation of the activated carbon with an acidic solution of $[PtCl_6]^{2-}$ ions at 298 K for 24 h. The water was evaporated at an increased temperature under vacuum. The catalyst was dried in air at 333 K for 12 h and then reduced in a hydrogen atmosphere for 2 h at 533 K.

The Pd-Pt-Bi/C catalyst was prepared by wet co-impregnation of the support with acidic solutions of $PtCl_2$, $PdCl_2$ and $Bi(NO_3)_3.5H_2O$. The activated carbon (AC) was previously washed with distilled water, filtered off and dried overnight at 333 K. The catalysts were impregnated with salt solutions and dried under vacuum. First, the salt precursor $Bi(NO_3)_3.5H_2O$ deposited on the support was decomposed upon heating under a nitrogen stream at 723 K during 18 h. Then, the catalysts were reduced under a hydrogen atmosphere. The system was heated with a ramp rate of 5 K/min until 533 K, with a hydrogen flow of 60 cm^3/min and then was kept under isothermal conditions for 5 hours.
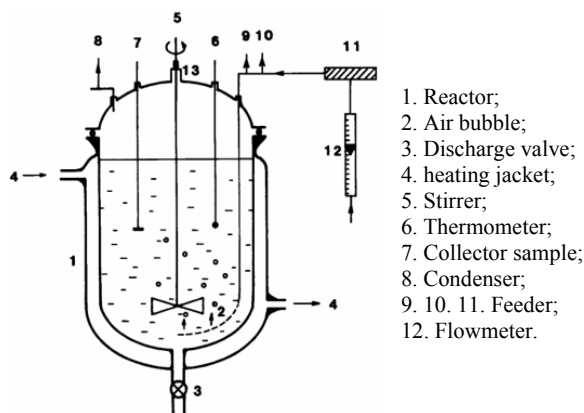
Catalysts Characterization

The X-ray diffraction (XRD) analyses of the catalysts were performed using a Rigaku DMAX model 2400 X-ray diffractometer (Cu Kα radiation, 40 kV, 20 mA). Diffraction data was recorded using a continuous scanning at 0.02°/s, step 0.02°. The crystalline phases were identified by reference to the JCPDS data file. The chemical composition of the samples was determined by X-ray fluorescence analysis (XRF), using a Rigaku spectrometer, model Rix 3100, controlled by software Rix 3100, with an X-ray tube of Rh anode. The textural characteristics, specific surface area and pore volume (BJH method) were determined by N_2 physisorption at 77 K in a Micromeritics ASAP 2020.

Acid sites of the support were identified by the results of the determination of superficial groups by Boehm titrations with $NaHCO_3$, NaOH, Na_2CO_3 for carboxylic, phenolic and lactonic groups, respectively (Boehm, 1994, 2002).

Oxidation Experiments

The glycerol oxidation experiments were performed in a borosilicate glass reactor of the mechanically agitated slurry reactor (MASR) type (Figure 1) equipped with a two-bladed turbine-type impeller mixer.

1. Reactor;
2. Air bubble;
3. Discharge valve;
4. heating jacket;
5. Stirrer;
6. Thermometer;
7. Collector sample;
8. Condenser;
9. 10. 11. Feeder;
12. Flowmeter.

Figure 1: Scheme of the mechanically agitated slurry reactor (MASR).

The system was operated in batch mode for the solid and liquid phases under continuous gas flow during 4 hours. First, the Pt(3.0 wt.%)/C catalyst was evaluated in terms of the glycerol conversion with selectivities in acids. Then, a commercial trimetallic (Pt-Pd-Bi/C) catalyst, supplied by Evonik (USA), was tested as a reference for glycerol conversion by selective oxidation to acids. Based on the results obtained, the Pt-Pd-Bi catalyst with low content of metals (3.2% weight) was evaluated.

An aqueous solution of glycerol (1.08 M, 700 cm^3) was prepared and mixed with NaOH at the molar ratio [NaOH]/[glycerol] =1.5. Catalyst was added in masses of 5 and 10 g. Oxygen was bubbled through the solution at a constant flow rate of 43 dm^3/h through a valve located at the top of the reactor. Atmospheric pressure (1.0 bar) was maintained. A thermal sensor in the reactor and an external heating element controlled the temperature at 333 K with the accuracy of ±1.0 K.

Analyses of the Reaction

The samples taken each 30 min were analyzed by High Performance Liquid Chromatography (RI detector, Waters, USA). The separation was performed with an Aminex HPX 87H column at 323 K with 0.005 M aqueous sulfuric acid solution (0.6 cm^3/min) as eluent. The identification and quantification of the reactant and products (glycerol, glyceric acid, tartronic acid, glycolic acid, oxalic acid) were done by comparison with standard solutions.

RESULTS AND DISCUSSION

Characterization of Catalysts

The diffractograms of the trimetallic Pd(4.0 wt.%)-Pt(1.0 wt.%)-Bi(5.0 wt.%)/C commercial catalyst from Evonik and of the Pd(0.2 wt.%)-Pt(1.0 wt.%)-Bi(2.0 wt.%) catalyst prepared from inorganic ligands indicated the presence of metallic Pd(2θ=40.1). The XRD analysis showed the presence of an intermetallic compound with the composition BiPd$_3$(2θ=28.5), metallic bismuth(2θ=24.6) and minor amounts of Bi$_2$O$_3$ (2θ=30.3). Moreover, XRD characterization of the monometallic Pt/C and trimetallic Pd-Pt-Bi/C catalysts prepared confirmed the presence of metallic Pt(2θ = 39.8).

The chemical composition of the constituent metal components determined by X-ray fluorescence (XRF) analyses was found to be Pd:Pt:Bi: 0.18:1.00:1.95 for the trimetallic catalyst prepared and Pd:Pt:Bi: 3.80: 1.00:4.70 for the commercial catalyst. The error associated with the analysis was ±0.01. The surface area measurements showed that deposition of the precursors on the support initially caused a decrease in surface area, followed by an increase after their thermal decomposition. The values of the BET surface areas of the Pd-Pt-Bi/C and Pt/C are presented in Table 1.

Acid functional groups on the support surface, determined by Boehm titrations, presented 0.051 mEq.g^{-1} of lactonic acid groups and 0.352 mEq.g^{-1} of phenolic acid groups.

Table 1: Surface area of catalysts.

Catalyst	S_{BET} (m^2/g)
Pd(4.0 wt.%)-Pt(1.0 wt.%)-Bi(5.0 wt.%)/C	930
Pd(0.2 wt.%)-Pt(1.0 wt.%)-Bi(2.0 wt.%)/C	640
Pt(3.0 wt.%)/C	680

The process was initially evaluated with the monometallic platinum catalyst, then, to obtain improved conditions of acid production, the catalyst formulated with platinum, palladium and bismuth was tested.

Oxidation of Glycerol with Platinum Catalyst

Oxidation experiments were carried out in alkaline conditions using Pt(3.0 wt.%)/C catalyst at

313 K and 333 K, under 1.0 bar. The reactant (glycerol, GLY) and the products (glyceric acid, GCA; tartronic acid, TTA; glycolic acid, GLYCA; oxalic acid, OXA; dihydroxyacetone, DHA) were analyzed by HPLC with satisfactory separation resolutions. The influence of the temperature of reaction was analyzed. The results of the operation at 333 K are shown in Figure 2.

The platinum catalyst Pt(3.0 wt.%)/C presented a high activity for the oxidation process, reaching 99.1% of glycerol conversion at 4 hr of reaction time, at 333 K. The main products were glyceric and tartronic acids, while other compounds were obtained in low concentration and could be considered as by-products. The reaction operations performed at 313 K, under the same conditions, presented results that were comparable in terms of conversion (X_{GLY} = 100x(C_{GLY0} − C_{GLY})(C_{GLY0})$^{-1}$) and selectivity (S_i = 100x C_i(C_{GLY0} − C_{GLY})$^{-1}$; i = acids, DHA) with those obtained at 333 K (Table 2).

It was observed that the catalyst containing platinum provided a high conversion, but low selectivities in acids. Fordham *et al*. (1995) indicated the use of other metals acting as promoters to increase the selectivity in acids. Thus, the catalyst formulated as Pd(4.0 wt.%)-Pt(1.0 wt.%)-Bi(5.0 wt.%)/C, supplied by Evonik, USA, was tested. Figure 3 presents the evolution of the concentrations of the components of the oxidation processed at 333 K with the commercial trimetallic catalyst. The glycerol was pratically all converted (98%) after 4 hr (Figure 3), and a significant production of glyceric acid was obatined, higher than that obtained with the monometallic catalyst Pt(3.0 wt.%)/C.

The conversions of glycerol and the product selectivities at the temperatures 333 K and 313 K obtained with the catalyst Pd(4.0 wt.%)-Pt(1.0 wt.%)-Bi(5.0 wt.%)/C are compared in Table 3. It was observed that the temperature influenced directly the selectivity of glyceric acid, which decreased from 62.7% at 313 K to 46.3% at 333 K.

Considering the activity obtained with the catalyst provided by Evonik (USA), the evaluation of the catalyst formulated as Pd(0.2 wt.%.) - Pt(1.0 wt.%) – Bi(2.0 wt.%)/C was performed. In this case, oxygen was supplied by atmospheric air. The results in terms of the concentrations of the reactant and products are shown in Figure 4.

The formulated catalyst presented high conversion and selectivity (Table 4), similar to those of the catalyst produced by Evonik. However, it was more selective for the oxidation of the primary OH group, producing mainly the glyceric acid.
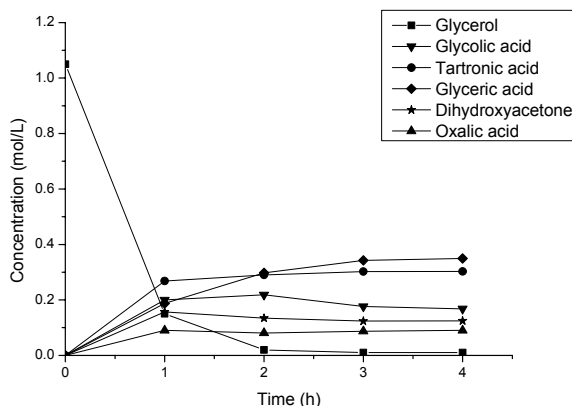
Figure 2: Concentration profiles of reactant and products of oxidation of glycerol. Reaction conditions: catalyst Pt(3.0 wt.%)/C, 10 g, initial concentration 1.08 M, molar feed ratio [NaOH]/[glycerol] = 1.5, 333 K, P_{O_2} = 1.0 bar, 500 rpm.

Table 2: Conversion of glycerol and selectivity of acids. Effect of temperature. Reaction conditions: catalyst Pt(3.0 wt.%)/C, 10 g, initial concentration 1.08 M, molar feed ratio [NaOH]/[glycerol] = 1.5, P_{O_2} = 1.0 bar, 500 rpm, reaction time 4 hr.

Temperature(K)	S_{OXA}(%)	S_{TTA}(%)	S_{GCA}(%)	S_{GLYCA}(%)	S_{DHA}(%)	X_{GLY}(%)
313	6.2	29.8	30.1	19.7	14.3	98.8
333	8.7	29.4	33.8	16.2	11.9	99.1
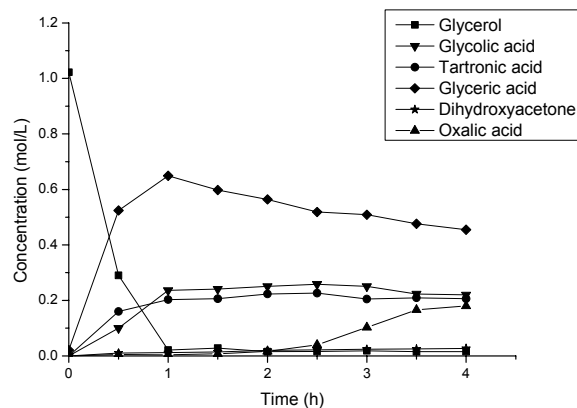
Figure 3: Concentration profiles of reactant and products of oxidation of glycerol. Reaction conditions: catalyst Pd(4.0 wt.%)-Pt(1.0 wt.%)-Bi(5.0 wt.%)/C-Evonik, 10 g, initial concentration 1.08 M, molar feed ratio [NaOH]/[glycerol] = 1.5, 333 K, P_{O_2} = 1.0 bar, 500 rpm.

Table 3: Conversion of glycerol and selectivity of acids. Effect of temperature. Reaction conditions: catalyst Pd(4.0 wt.%)-Pt(1.0 wt.%)-Bi(5.0 wt.%)/C (Evonik, USA), 10 g, initial concentration 1.08 M glycerol, molar [NaOH]/[glycerol] = 1.5, P_{O_2} = 1.0 bar, 500 rpm, reaction time 4 hr.

Temperature(K)	S_{OXA}(%)	S_{TTA}(%)	S_{GCA}(%)	S_{GLYCA}(%)	S_{DHA}(%)	X_{GLY}(%)
313	6.3	19.1	62.7	10.9	< 1.0	92.2
333	13.9	20.9	46.3	16.9	2.0	98.0
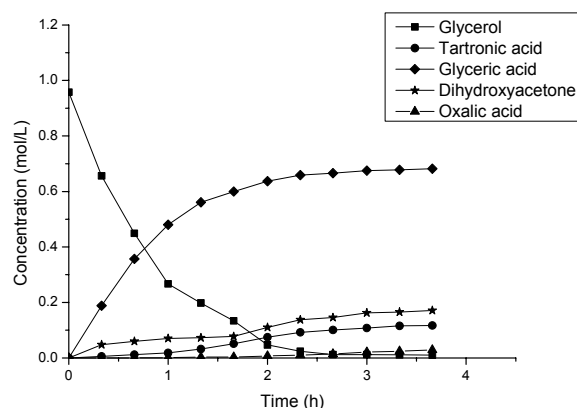
Figure 4: Concentration profiles of reactant and products of oxidation of glycerol. Reaction conditions: catalyst Pd(0.2 wt.%)-Pt(1.0 wt.%)- Bi(2.0 wt.%)/C, 5.0 g, initial concentration 1.08 M, molar feed ratio [NaOH]/[glycerol] = 1.5, 333 K, P_{Air} = 1.0 bar, 500 rpm.

Table 4: Conversion of glycerol and selectivity of acids. Effect of temperature. Reaction conditions: catalyst Pd(0.2 wt.%)-Pt(1.0 wt.%)- Bi(2.0 wt.%)/C, 5.0 g, initial concentration 1.08 M glycerol, molar [NaOH]/[glycerol] = 1.5, P_{Air} = 1.0 bar, 500 rpm, reaction time 4 hr.

Temperature(K)	S_{OXA}(%)	S_{TTA}(%)	S_{GCA}(%)	S_{GLYCA}(%)	S_{DHA}(%)	X_{GLY}(%)
313	3.2	7.1	80.1	< 1.0	8.5	83.5
333	2.1	11.0	70.6	< 1.0	15.3	98.9

Kinetic Modeling

Based on the experimental evidence obtained with Pt(3.0 wt.%)/C and Pd(4.0 wt.%)-Pt(1.0 wt.%)-Bi(5.0 wt.%)/C catalysts, and the indications made by Worz *et al*. (2009), a reaction network was assumed (Scheme 1). According to the proposal, the oxidation of the primary OH group of glycerol (GLY) leads mainly to glyceric acid (GLYA), followed by tartronic acid (TTA). Through the oxidation of the secondary OH group of glycerol, dihydroxyacetone (DHA) was obtained, and then converted into oxalic acid (OXA).

The reaction network assumed allowed the formulation of a simplified network (Scheme 2). The simplified mechanism considers only the chemisorption of oxygen and adsorption of glycerol and acid products formed by oxidation. Intermediates whose yields were very small are neglected.

Based on the Langmuir-Hinshelwood approach, the kinetic model was formulated considering the glycerol oxidation network (Scheme 1). It was considered that glycerol and acids compete with each other for the same metallic sites, while molecular oxygen was adsorbed on the acid sites of the support. It was assumed that the adsorption of the products was weaker than that of glycerol, which was adsorbed with moderate intensity.

The detailed reaction steps are indicated in Table 5, with the corresponding reaction rate expressions.

In these expressions, r_i and k_i (i = reaction steps) are the reaction rates and the constant reaction rates, respectively. Θ_j are the fractions of the occupied sites, where j = glycerol, acids.

$$r_i = \frac{k_i K_j K_{O_2} C_j C_{O_2}}{(1 + K_{GLY} C_{GLY} + \sum_{j_P} K_{j_P} C_{j_P})(1 + K_{O_2} C_{O_2})} \quad (1)$$

C_j are the concentrations of the reaction components and K_j the corresponding adsorption equilibrium constants. Considering that product adsorption should be weaker than that of glycerol, it was assumed that: $\sum_{j_P} K_{j_P} C_{j_P} << 1 + K_{GLY} C_{GLY}$; j_p = products.

The experiments were carried out with oxygen in excess, so that k'_{ij} ($k'_{ij} = \dfrac{k_i K_j K_{O_2} C_{O_2}}{(1 + K_{O_2} C_{O_2})}$) can be identified as pseudo-kinetic constants. Thus, the reaction rates can be written as:

$$r_i = \frac{k'_{ij} C_j}{(1 + K_{GLY} C_{GLY})} \quad (2)$$

Under the operating conditions, in order to confirm the rate-controlling regime in the catalytic reaction steps, the mass transfer limitations through the Weisz criterion, Φ'_{GLY} ($\Phi'_{GLY} = r_{GLYexp}(d_p/6)^2$ $(D_{eGLY} C_{GLY})^{-1}$, and the external mass transfer resistance fraction f_{eGLY} ($f_{eGLY} = r_{GLYexp}(d_p/6)$ $(k_{GLYm} C_{GLY})^{-1}$ were quantified (Villermaux, 1993). The estimated values $\Phi'_{GLY} = 2.34x10^{-2} \to 0$; $f_{eGLY} = 1.73x10^{-3} << 0.05$ show that the process was rate-controlling, indicating that there were no mass transfer limitations.
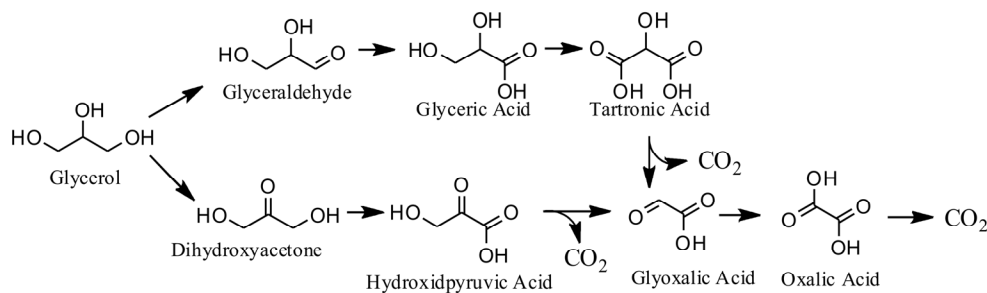
Scheme 1: Reaction network of the glycerol oxidation (Worz *et al*., 2009).
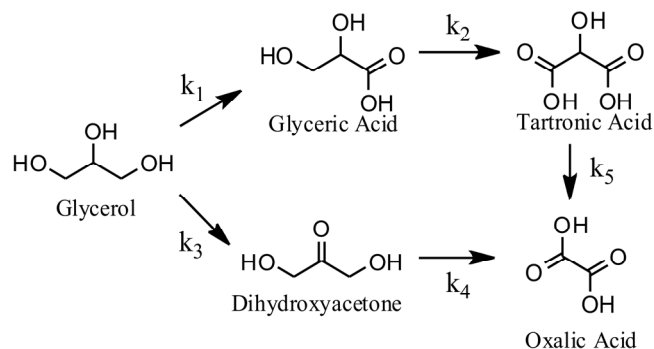
Scheme 2: Simplified reaction network for the catalytic oxidation of glycerol in alkaline medium.

Table 5: Glycerol oxidation steps.

Adsorption Step	Reaction step	Reaction rate	Adsorption equilibrium constant
$GLY + A \underset{k_{-1,d}}{\overset{k_{1,ad}}{\rightleftharpoons}} GLY.A$	-	-	$K_G = \dfrac{k_{1,ad}}{k_{-1,d}}$
$O_2 + AC^* \underset{k_{-2,d}}{\overset{k_{2,ad}}{\rightleftharpoons}} O_2.AC^*$	$GLY.A + O_2.AC^* \xrightarrow{k_1} GCA.A$ $GLY.A + O_2.AC^* \xrightarrow{k_3} DHA.A$	$r_1 = k_1 \Theta_{GLY} \Theta_{O_2}$ $r_3 = k_3 \Theta_{GLY} \Theta_{O_2}$	$K_{O_2} = \dfrac{k_{2,ad}}{k_{-2,d}}$
$GCA.A \underset{k_{-3,d}}{\overset{k_{3,ad}}{\rightleftharpoons}} GCA + A$	$GCA.A + O_2.AC^* \xrightarrow{k_2} TTA.A$	$r_2 = k_2 \Theta_{GCA} \Theta_{O_2}$	$K_{GCA} = \dfrac{k_{3,ad}}{k_{-3,d}}$
$TTA.A \underset{k_{-5,d}}{\overset{k_{5,ad}}{\rightleftharpoons}} TTA + A$	$TTA.A + O_2.AC^* \xrightarrow{k_5} OXA.A$	$r_5 = k_5 \Theta_{TTA} \Theta_{O_2}$	$K_{TTA} = \dfrac{k_{4,ad}}{k_{-4,d}}$
$DHA.A \underset{k_{-5,d}}{\overset{k_{5,ad}}{\rightleftharpoons}} DHA + A$	$DHA.A + O_2.AC^* \xrightarrow{k_4} OXA.A$	$r_4 = k_4 \Theta_{DHA} \Theta_{O_2}$	$K_{DHA} = \dfrac{k_{5,ad}}{k_{-5,d}}$
$OXA.A \underset{k_{-6,d}}{\overset{k_{6,ad}}{\rightleftharpoons}} OXA + A^*$	-	-	$K_{OXA} = \dfrac{k_{6,ad}}{k_{-6,d}}$
$OXA.A \underset{k_{-7,d}}{\overset{k_{7,ad}}{\rightleftharpoons}} OXA + A^{**}$	-	-	$K_{OXA} = \dfrac{k_{7,ad}}{k_{-7,d}}$

* *OXA* from *DHA*; ** *OXA* from *TTA*; A metal site; AC^* support site.

The mass balance equations of the reaction components of the liquid phase are presented in Table 6.

The solution of the mass balance equations was obtained by the fourth-order Runge-Kutta method (MATLAB.ode45s subroutine) and the subroutine hybrid fractional error function (HYBRID) was used to obtain the best-fit between the calculated (C_j^{cal}) and the experimental data (C_j^{Exp}). The initializing values of the reaction rate constants and adsorption coefficients employed in the optimization procedure were obtained by a differential method and the indications of Hu *et al*. (2011). The optimization procedure was performed with the data of each isothermal operation and the values of the kinetic parameters (Table 7) and adsorption equilibrium constants were estimated at 313 K, 323 K and 333 K. To confirm the results, the same procedure was applied for the set of experimental data obtained at the three temperatures. Then, Arrhenius and van't Hoff laws were introduced and the parameters E_{act} and ΔH_{ads} were optimized (Table 8). The activation energy and heat of adsorption values obtained are of the same order as those found by Hu *et al*. (2011).

An objective function was defined as: $f_{Oj} = \sum (C_j^{Exp} - C_j^{Cal})^2$, for the data of each component of the process. The experimental data were well predicted by the model, with agreement with the objective function between 10^{-3} and 10^{-2}.

Experimental and predicted data obtained at 313 K, 323 K and 333 K are shown in Figures 5 - 7.

**Table 6: Mass balance equations of the reaction components. $w = m_{cat}/V_L$.**

Component	Mass balance equation	
GLY	$\dfrac{1}{w}\dfrac{dC_{GLY}}{dt} = r_1 - r_3$	$\dfrac{1}{w}\dfrac{dC_{GLY}}{dt} = -\dfrac{(k'_{1GLY} + k'_{3GLY})C_{GLY}}{(1 + K_{GLY}C_{GLY})}$
GCA	$\dfrac{1}{w}\dfrac{dC_{GCA}}{dt} = r_1 - r_2$	$\dfrac{1}{w}\dfrac{dC_{GCA}}{dt} = \dfrac{k'_{1GLY}C_{GCA} - k'_{2GCA}C_{GCA}}{(1 + K_{GLY}C_{GLY})}$
DHA	$\dfrac{1}{w}\dfrac{dC_{DHA}}{dt} = r_3 - r_4$	$\dfrac{1}{w}\dfrac{dC_{DHA}}{dt} = \dfrac{k'_{3GLY}C_{DHA} - k'_{4DHA}C_{DHA}}{(1 + K_{GLY}C_{GLY})}$
TTA	$\dfrac{1}{w}\dfrac{dC_{TTA}}{dt} = r_2 - r_5$	$\dfrac{1}{w}\dfrac{dC_{TTA}}{dt} = \dfrac{k'_{2GCA}C_{GCA} - k'_{5TTA}C_{TTA}}{(1 + K_{GLY}C_{GLY})}$
OXA	$\dfrac{1}{w}\dfrac{dC_{OXA}}{dt} = r_4 + r_5$	$\dfrac{1}{w}\dfrac{dC_{OXA}}{dt} = \dfrac{k'_{4DHA}C_{DHA} + k'_{5TTA}C_{TTA}}{(1 + K_{GLY}C_{GLY})}$

Table 7: Reaction rate constants. Conditions: catalyst Pt(1.0 wt.%)-Pd(0.2 wt.%)-Bi(2.0 wt.%)/C, molar feed ratio [NaOH]/[glycerol] = 1.5, P_{O_2} = 1.0 bar, 500 rpm.

Reaction step	Reaction rate constant, k_i (mol/dm³.min)		
	313 K	323 K	333 K
$GLY.A + O_2.AC^* \xrightarrow{k_1} GCA.A$	1.67×10^{-2}	2.64×10^{-2}	4.06×10^{-2}
$GCA.A + O_2.AC^* \xrightarrow{k_2} TTA.A$	1.22×10^{-3}	1.67×10^{-3}	2.25×10^{-3}
$GLY.A + O_2.AC^* \xrightarrow{k_3} DHA.A$	2.01×10^{-3}	4.07×10^{-3}	7.92×10^{-2}
$DHA.A + O_2.AC^* \xrightarrow{k_4} OXA.A$	1.53×10^{-3}	4.06×10^{-3}	1.01×10^{-2}
$TTA.A + O_2.AC^* \xrightarrow{k_5} OXA.A$	1.34×10^{-2}	1.59×10^{-2}	1.88×10^{-2}

Table 8: Activation energies and heats of adsorption Conditions: catalyst Pd(0.2 wt.%)-Pt(1.0 wt.%)- Bi(2.0 wt.%)/C, molar feed ratio [NaOH]/[glycerol] = 1.5, 313 - 333 K, P_{Air} = 1.0 bar, 500 rpm, reaction time 4 hr.

Reaction step	E_{ai} (kJ/mol)	Component	$-\Delta H_i$ (kJ/mol)
Glycerol → Glyceric acid	38.5	Glycerol	7.24
Glyceric acid → Tartronic acid	26.3	Glyceric acid	99.3
Glycerol → Dihydroxyacetone	59.6	Tartronic acid	39.7
Dihydroxyacetone → Oxalic acid	81.9	Dihydroxyacetone	59.6
Tartronic acid → Oxalic acid	14.6		
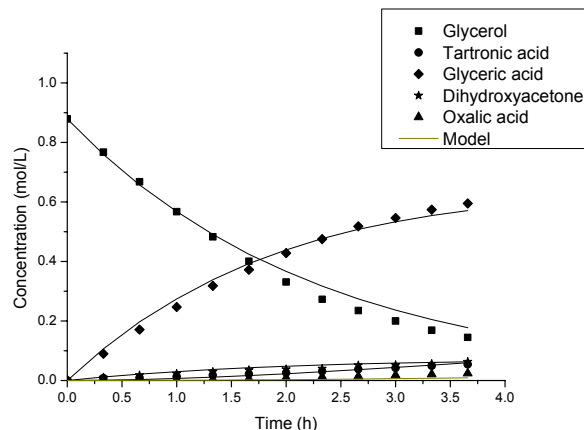
Figure 5: Experimental and predicted concentration profiles of reactant and products of oxidation of glycerol. Conditions: catalyst Pd(0.2 wt.%)-Pt(1.0 wt.%)- Bi(2.0 wt.%)/C, 5.0 g, initial concentration 1.08 M, molar feed ratio [NaOH]/ [glycerol] = 1.5, 313 K, P_{Air} = 1.0 bar, 500 rpm.
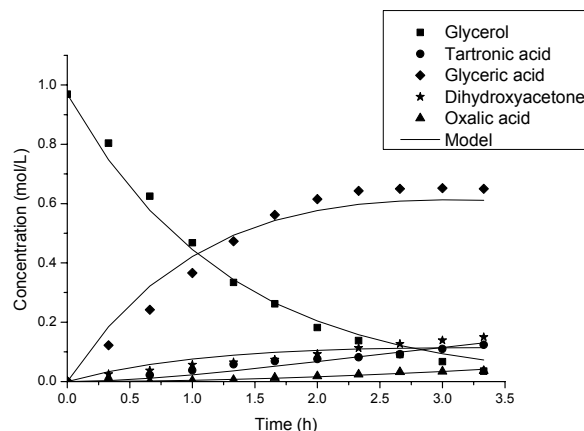
Figure 6: Experimental and predicted concentration profiles of reactant and products of oxidation of glycerol. Conditions: catalyst Pd(0.2 wt.%)-Pt(1.0 wt.%)- Bi(2.0 wt.%)/C, 5.0 g, initial concentration 1.08 M, molar feed ratio [NaOH]/ [glycerol] = 1.5, 323 K, P_{Air} = 1.0 bar, 500 rpm.
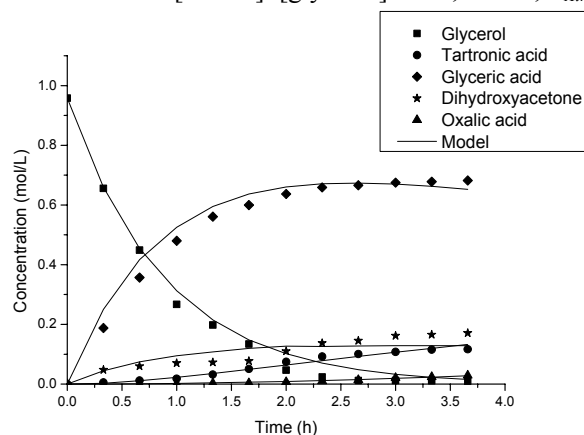
Figure 7: Experimental and predicted concentration profiles of reactant and products of oxidation of glycerol. Conditions: catalyst Pd(0.2 wt.%)-Pt(1.0 wt.%)- Bi(2.0 wt.%)/C, 5.0 g, initial concentration 1.08 M, molar feed ratio [NaOH]/[glycerol] = 1.5, 333 K, P_{Air} = 1.0 bar, 500 rpm.

The values of the rate constants for the steps of production of glyceric acid and dihydroxyacetone were slightly higher for this acid production step. The predominance of this step was confirmed by the magnitude of their activation energies. The production of dihydroxyacetone occurred with an activation energy about 1.5 times higher than that of the production of glyceric acid.

Considering the consecutive reaction steps (Scheme 2) and their activation energies, it was indicated that the production of oxalic acid occurred mainly via tartronic acid.

Adsorption equilibrium constants for glycerol were in the range of 5.77 x10^{-4} – 4.88x10^{-4} dm^3/mol, while for the products (glyceric and tartronic acids, dihydroxyacetone) the orders of magnitude were from 1.30x10^{-18} to 9.71x10^{-10} dm^3/mol.

These results would appear to confirm the hypotheses considered in the formulation of the model,

including moderate adsorption of glycerol and weak adsorption of the products.

CONCLUSIONS

Glycerol oxidation was performed in this work using monometallic and trimetallic catalysts in a MASR reactor, presenting as products glyceric acid, tartronic acid, glycolic acid, oxalic acid and dihydroxyacetone. The selectivity for glyceric acid in this process was greatly improved by use of the trimetallic catalyst Pd(0.2 wt.%)-Pt(1.0 wt.%)-Bi(2.0 wt.%)/C to enhance the oxidation of the primary OH group, reaching higher selectivity than with the catalyst containing only platinum on the support.

The kinetics of glycerol oxidation were studied using the trimetallic catalyst Pd(0.2 wt.%)-Pt(1.0 wt.%)-Bi(2.0 wt.%)/C, and a simplified network was

proposed based on the Langmuir-Hinshelwood mechanism. This simplified network was investigated and the kinetic and adsorption equilibrium parameters were obtained and related to the tendency for selective formation of acid glyceric, which presented the lowest value of activation energy (38.5 kJ/mol) for its production step and the highest adsorption equilibrium constant for the reactant glycerol (10^{-4} dm^3/mol).

ACKNOWLEDGMENTS

NOMENCLATURE

A	active site on the surface of the catalyst	
AC	activated carbon	
C_j	concentrations of the reaction components	mol/dm^3
C_j^{Cal}	calculated concentration of each component	mol/dm^3
$C^{Exp}-$	experimental concentration of each component	mol/dm^3
C_{GLY}	concentration of glycerol	mol/dm^3
C_{GLY0}	initial concentration of glycerol	mol/dm^3
DHA	dihydroxyacetone	
d_p	particle diameter	m
D_{eGLY}	diffusivity	m^2/s
E_a	activation energy	kJ/mol
f_{eGLY}	external mass transfer fraction	
GCA	glyceric acid	
GLA	glyceraldehyde	
GLY	glycerol	
GLYCA	glycolic acid	
GOX	glyoxalic acid	
HPA	hydroxypyruvic acid	
j_p	products	
k_{GLYm}	mass transfer coefficient of glycerol	m/s
K_j	equilibrium constant of adsorption/desorption on active sites	atm^{-1} for oxygen and dm^3/mol for other species
k	rate constant	mol/dm^3.min
OXA	oxalic acid	

P_{Air}	air pressure	atm
P_{O_2}	oxygen pressure	atm
r	reaction rate	mol/dm^3.min
$r_{GLY\exp}$	experimental reaction rate of glycerol	mol/dm^3.s
S	selectivity	
TTA	tartronic acid	
w	catalyst weight	g
X	conversion	
Φ	Thiele's module	
Θ	fractions of the occupied sites	
$\Delta H_{ad,j}$	enthalpy of adsorption	kJ/mol
[ ]	concentration of component	mol/dm^3

Subscripts

i	step
j	glycerol, acids

REFERENCES

Alardin, F., Ruiz, P., Delmonb, B. and Devillers, M., Bismuth-promoted palladium catalysts for the selective oxidation of glyoxal into glyoxalic acid. Appl. Catal. A: General, 215, 125-136 (2001).

Behr, A., Eilting, J., Irawaldi, K., Leschinski, J. and Lindner, F., Improved utilization of renewable resources: New important derivatives of glycerol. Green Chem., 10, 13 (2008).

Boehm, H. P., Some aspects of the surface chemistry of carbon blacks on other carbons. Carbon, 32, 759-769 (1994).

Boehm, H. P., Surface oxides on carbon and their analysis: A critical assessment. Carbon, 40, 145-149 (2002).

Carrettin, S., McMorn, P., Johnston, P. Griffin, K., Kiely, C. J. and Hutchings, G. J., Oxidation of glycerol using supported Pt, Pd and Au catalysts. Phys. Chem. Chem. Phys., 5, 1329-1336 (2003).

Corma, A., Iborra, S. and Velty, A., Chemical routes for the transformation of biomass into chemicals. Chem. Rev., 107, 2411-2502 (2007).

Demirel-Gülen, S., Lucas, M. and Claus, P., Liquid phase oxidation of glycerol over carbon support gold catalysts. Catal. Today, 102-103,166-172 (2005).

Demirel, S., Lucas, M., Warna, J., Salmi, T., Murzin, D. and Claus, P., Reaction kinetics and modeling of the gold catalysed glycerol oxidation. Top. Catal., 44, 299-305 (2005).

Ferretti, C. A., Soldano, A., Apesteguía, C. R. and Cosimo, J. I. Di, Monoglyceride synthesis by glycerolysis of methyl oleate on solid acid-base. Chem. Eng. J., 161, 346-354 (2010).

Fordham, P., Besson, M. and Gallezot, P., Selective catalytic oxidation of glyceric acid to tartronic and hydroxypyruvic acids. Appl. Catal. A: General, 133,179-184 (1995).

Gallezot, P., Selective oxidation with air on metal catalysts. Catal. Today, 37, 405-418 (1997).

Guo, L., Zhou, J., Mao, J., Guo, X. and Zhang, S., Supported Cu catalysts for the selective hydrogenolysis of glycerol to propanediols. Appl. Catal. A: Chem., 367, 93-98 (2009).

Hu, W., Lowry, B. and Varma, A., Kinetic Study of Glycerol Oxidation Network over Pt-Bi/C Catalyst. Appl. Catal. B: Environmental, 106, 123-132 (2011).

Ketchie, W. C., Murayama, M. and Davis, R. J., Promotional effect of hydroxyl on the aqueous phase oxidation of carbon monoxide and glycerol over supported Au catalysts. Top. Catal., 44, 307-317 (2007a).

Ketchie, W. C., Murayama, M. and Davis, R. J., Selective oxidation of glycerol over carbon-supported AuPd catalysts. J. of Catalysis, 250, 264-273 (2007b).

Kimura, H., Tsuto, K., Wakisaka, T., Kazumi, Y. and Inaya, Y., Selective oxidation of glycerol on a platinum-bismuth catalyst. Appl. Catal. A: Gen., 96, 217-228 (1993).

Kimura, H., Selective oxidation of glycerol on a platinum-bismuth catalyst by using a fixed bed reactor. Appl. Catal. A: Gen., 105, 147-158 (1993).

Lehr, V., Sarlea, M., Ott, L. and Vogel, H., Catalytic dehydration of biomass-derived polyols in sub- and supercritical water. Catal. Today, 121, 121-129 (2007).

Luo, N., Fu, X., Cao, F., Xiao, T. and Edwards, P. P., Luo, N., Fu, X., Cao, F., Xiao, T. and Edwards, P. P., Glycerol aqueous phase reforming for hydrogen generation over Pt catalyst – Effect of catalyst composition and reaction conditions. Fuel, 87, 3483-3489 (2008).

Mallat, T. and Baiker, A., Catalyst potential: A key for controlling alcohol oxidation. Catal. Today, 24, 143-150 (1995).

McCoy, M., Glicerin surplus. Chem. Eng. News, 84, 7 (2006).

Tullo, A. H., A living plant. Chem. Eng. News, 85, 53 (2007).

Verde, Y., Alonso, G., Zhang, R. V. H., Jacobson, A. J. and Keer, A., Pt/C obtained from carbon with different treatments and $(NH_4)_2PtCl_6$ as a Pt precursor. Appl. Catal. A: Gen., 277, 201-207 (2004).

Villermaux, J., Génie de la réaction chimique conception et fonctionnement des réacteurs. Technique et Documentation Lavoisier, Paris (1993). (In French).

Worz, N., Brandner, A., Claus, P., Platinum-Bismuth-catalyzed oxidation of glycerol: Kinetics and the origin of selective deactivation. J. Phys. Chem. C, 114, 1164-1172 (2009).